Avrupa Bilim ve Teknoloji Dergisi
Özel Sayı 43, S. 126-135, Kasım 2022

Araştırma Makalesi

www.ejosat.com ISSN:2148-2683

European Journal of Science and Technology
Special Issue 43, pp. 126-135, November 2022

Research Article

Structural Analysis of the Nose Landing Gear of a Fighter Aircraft

Gözde Aydın[1*], İbrahim Özkol[2]

[1*] İstanbul Technical University, Departmant of Aeronautics and Astronautics Engineering, İstanbul, Turkey, (ORCID: 0000-0003-0142-2056), aydingo@itu.edu.tr
[2] İstanbul Technical University, Aerospace Research Center, İstanbul, Turkey, (ORCID: 0000-0002-9300-9092), ozkol@itu.edu.tr

(4th International Conference on Applied Engineering and Natural Sciences ICAENS 2022, November 10 - 13, 2022)

(**DOI:** 10.31590/ejosat.1200620)

ATIF/REFERENCE: Aydın, G., Ozkol, I. (2022). Structural Analysis of the nose Landing Gear of a Fighter Aircraft. *European Journal of Science and Technology*, (43), 126-135.

Abstract

The landing gear, which is one of the most important mechanical systems in aircraft, is the structure that is exposed to landing loads, one of the most important and critical loads that the aircraft is exposed to throughout its life cycle. In addition to the fact that the landing gear system must have high strength to these loads, long life, high performance, low volume, minimum weight, and low cost are important criteria. For this purpose, the optimum design is created by making a structural analysis using the landing gear finite element method. The main purpose of this study is to analyze the strength criteria by performing the structural analysis of the nose landing gear of a fighter aircraft. For the design, the most critical static and dynamic loads in the landing condition were calculated and applied as vertical, side, and drag forces. The displacement and stress values obtained as the final result by using metallic materials such as Aluminum 7075 T6 alloy, Titanium Ti-6Al-4V alloy, PH13-8Mo, 300M Steel, SAE 1035, and AISI 4340 steel alloy in the nose landing gear fork, torque links, side stay arms, and main strut were compared. The safety of the parts was examined from the results of the analysis. CAD drawings were made using Siemens NX and ANSYS SpaceClaim program. Structural analysis was applied with the ANSYS Workbench program, which uses the finite element method.

Keywords: Landing Gear, Static Structural, Materials, Stress, Deformation, ANSYS.

Bir Savaş Uçağının Burun İniş Takımının Yapısal Analizi

Öz

Uçaklardaki en önemli mekanik sistemlerden biri olan iniş takımı, uçağın yaşam döngüsü boyunca maruz kaldığı en önemli ve kritik yüklerden biri olan iniş yüklerine maruz kalan yapıdır. İniş takımı sisteminin bu yüklere karşı yüksek dayanıma sahip olmasının yanı sıra uzun ömür, yüksek performans, düşük hacim, minimum ağırlık ve düşük maliyet önemli kriterlerdendir. Bu amaçla iniş takımı sonlu elemanlar yöntemi kullanılarak yapısal analiz yapılır ve optimum tasarım oluşturulur. Bu çalışmanın temel amacı, bir savaş uçağının burun iniş takımının yapısal analizini yaparak mukavemet kriterlerini analiz etmektir. Tasarım için, iniş durumundaki en kritik statik ve dinamik yükler hesaplanmış ve düşey, yan ve sürükleme kuvvetleri olarak uygulanmıştır. Burun iniş takımı çatalı, tork bağlantıları, yan destek kolları ve ana dikmede, Alüminyum 7075 T6 alaşımı, Titanyum Ti-6Al-4V alaşımı, PH13-8Mo, 300M Çelik, SAE 1035 ve AISI 4340 çelik alaşımı gibi metalik malzemeler kullanılarak nihai sonuç olarak elde edilen deplasman ve gerilme değerleri karşılaştırıldı. Analiz sonuçlarından parçaların güvenliği incelenmiştir. CAD çizimleri Siemens NX ve ANSYS SpaceClaim programı kullanılarak yapılmıştır. Sonlu elemanlar yöntemini kullanan ANSYS Workbench programı ile yapısal analiz uygulanmıştır.

Anahtar Kelimeler: İniş Takımı, Statik Yapısal, Malzemeler, Gerilme, Deformasyon, ANSYS

1. Introduction

The landing gear is one of the most complex and critical systems in aircraft. One of the most basic tasks of the landing gear is to dampen the reaction forces coming to the aircraft during landing and take-off. Any damage to the landing gear while performing this function could result in a serious accident. Many different types of landing gear have been designed since the history of aviation. Currently, the most commonly used landing gear configuration is the tricycle landing gear. This landing gear is more stable in crosswinds and has good ground maneuverability. In addition, while fixed landing gears were used in the designs at first, it has been seen that this type of landing gear is disadvantageous in terms of aerodynamics over time. The retractable landing gear has been designed to meet the demands of higher speed and longer stay in the air. Although it is a more complex structure, the use of retractable landing gear has become widespread over time, considering the performance requirements in aircraft.

This change in the landing gear has advantages as well as disadvantages. Aerodynamically, the retractable landing gear is more efficient as it creates less drag than the fixed landing gear. However, the retractable landing gear has a more complex structure and is more weight. Weight is one of the most important elements in airplanes. By reducing its weight, more fuel can be added, thereby increasing airtime, or by reducing weight, adding more payload to the aircraft. Therefore, it is always desirable to reduce the weight of the aircraft. Landing gear makes up about 6% of the total weight of the aircraft. Designing landing gear with a high strength-to-weight ratio is the most important design requirement (Currey, 1988).

2. Geometry

First, the tricycle landing gear type was decided. Then, when deciding on the position of the main and nose landing gear, it should be ensured that the aircraft moves on the ground, does not roll over, reduces the side wind effect, and allows maneuverability during landing and take-off, taking into account the position of the center of gravity. The weight of the aircraft and the position range of the center of gravity constitute the main parameters in the design of the landing gear. Layout should be done by considering the clearance and tipping criteria. For this, the position of the center of gravity must be determined well. However, the position of the center of gravity changes under different conditions. Therefore, a certain allowable range for the center of gravity is specified. In the literature, this range is specified as a ratio of the mean aerodynamic chord (MAC), which indicates the length between the leading edge and trailing edge of the wing. The preferred center of gravity is in the range of 8% to 15% MAC (Conway, 1958).

The vertical distance between the landing gear attachment point to the aircraft and the landing gear contact point with the ground is called the landing gear height. The distance between the nose landing gear and the main landing gear is called the wheelbase. It is a parameter that affects the turning performance of the aircraft. Greater wheelbase means greater turning angle. It also affects the load distribution between the landing gear (Sadraey, 2012).

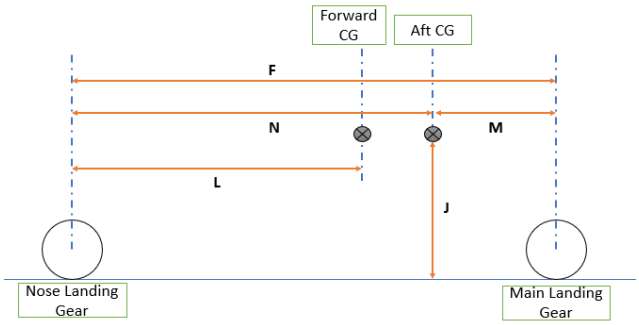

Figure 1 Landing Gear Layout

The values of the parameters indicating the landing gear arrangement shown in **Hata! Başvuru kaynağı bulunamadı.** are given in Table 1.

Table 1. Landing Gear Arrangement Parameters

F (mm)	L (mm)	N (mm)	M (mm)	J (mm)
4000	2590	2800	1200	1000

The main structural parts that make up the nose landing gear can be listed as rim, tire, oleo-pneumatic shock absorbing cylinder, wheel axle, wheel fork, links, side stay arm, main strut. The components of landing gear are shown in **Hata! Başvuru kaynağı bulunamadı.**.

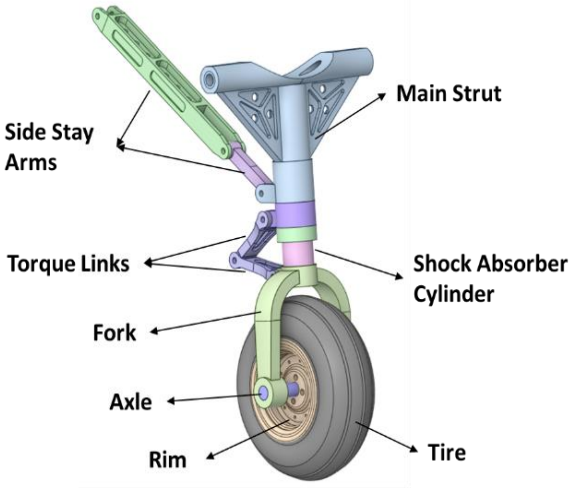

Figure 2 Landing Gear Components

3. Loads

The loadings to the landing gear are examined according to different landing conditions. For calculations, first of all, it is necessary to know the weight of the aircraft and the position of the landing gear relative to the aircraft's center of gravity. When the plane is in taxi, the wheels of the plane share the weight in certain proportions. This ratio is inversely proportional to the distance from the center of gravity. This result is obtained with the general moment equation. Considering this situation, the main landing gear is closer to the center of gravity and the nose landing gear is located further away. Considering the aircraft in the literature, when the nose landing gear and the main landing gear are evaluated by proportioning their distance from the center of gravity, it can be said that the nose landing gear carries about 5-20% of the load, and the main landing gear carries a load in the range of 80-95%. (Gudmundsson, 2014).

The critical forces acting on the landing gear under landing conditions can be listed as follows.

1- High drag force only when landing.

2- Normal drag and side force during landing.

3- Anti-drag forces by buckling of the strut under high frictional contact loads.

4- Forces due to brakes throughout the taxi.

5- Forces from rolling back.

6- Rotation and swing forces during taxi.

7- Sharp turning forces on the ground.

When calculating critical loading conditions, 80% of the take-off weight is used. A landing gear analysis will be performed for a fighter aircraft with a take-off weight of 16000 kg.

Formulas used for nose landing gear load:

$$N_1 = W_T\left(\frac{l_m + 0.4h}{l_m + l_n}\right)$$

W_T : Take-off weight.
l_m : Length between main landing gear and center of gravity.
l_n : Length between nose landing gear and center of gravity.
h : Height of the center of gravity from the ground.
N : Normal force.

$$N_2 = W_T\left(\frac{l_m + \frac{chD_B}{W_T}}{l_m + l_n}\right)$$

$D_B = \frac{4}{3}$ *(Drag corresponding to the maximum braking of the aircraft in motion)
c : Coefficient $= 2$

$$N_3 = \frac{1.75 * W_T * l_m}{l_m + l_n} + \frac{D_M h}{l_m + l_n}$$

$D_M = \frac{4}{3}$ *(Drag versus maximum braking of the aircraft on a main landing gear while in motion)

$$S = 0.25 \times N$$

S : Side force

$$D_1 = 0.4 \times N$$

D_1 : Drag force

$$D_2 = -0.7 \times N$$

D_2 : Drag force in rolling-back

The three most critical conditions for landing are three-point landing with high friction, taxing with brake and rolling-back. The forces were calculated for these three conditions using the above formulas.

4. Materials

The selected materials must be resistant to the incoming forces under loading conditions. Mechanical properties of materials are given in tables.

Table 2. Al 7075 T6 Mechanical Properties

Density (g/cm^3)	Young Modulus (MPa)	Poisson Ratio	Tensile Strength (MPa)	Yield Strength (MPa)
2.81	70960	0.33	572	503

Table 3. Ti-6Al-6V-2Sn Mechanical Properties

Density (g/cm^3)	Young Modulus (MPa)	Poisson Ratio	Tensile Strength (MPa)	Yield Strength (MPa)
4.54	110300	0.32	1050	980

Table 4. Ti 10V-2Fe-3Al Mechanical Properties

Density (g/cm^3)	Young Modulus (MPa)	Poisson Ratio	Tensile Strength (MPa)	Yield Strength (MPa)
4.65	110300	0.33	1430	1240

Table 5. Ti 6Al-4V Mechanical Properties

Density (g/cm^3)	Young Modulus (MPa)	Poisson Ratio	Tensile Strength (MPa)	Yield Strength (MPa)
4.43	113800	0.342	960	880

Table 6. PH13- 8Mo Mechanical Properties

Density (g/cm^3)	Young Modulus (MPa)	Poisson Ratio	Tensile Strength (MPa)	Yield Strength (MPa)
7.80	221000	0.28	1480	1415

Table 7. AISI 1035 Mechanical Properties

Density (g/cm^3)	Young Modulus (MPa)	Poisson Ratio	Tensile Strength (MPa)	Yield Strength (MPa)
7.87	196000	0.29	620	550

Table 8. 300M Steel Mechanical Properties

Density (g/cm^3)	Young Modulus (MPa)	Poisson Ratio	Tensile Strength (MPa)	Yield Strength (MPa)
7.83	205000	0.28	1931	1586

Table 9. AISI 4340 Mechanical Properties

Density (g/cm^3)	Young Modulus (MPa)	Poisson Ratio	Tensile Strength (MPa)	Yield Strength (MPa)
7.7	200000	0.29	1792	1496

5. Methods

The landing gear was analyzed by static analysis in the ANSYS Workbench program. The flow chart of the modelling process is shown in the Figure 3.

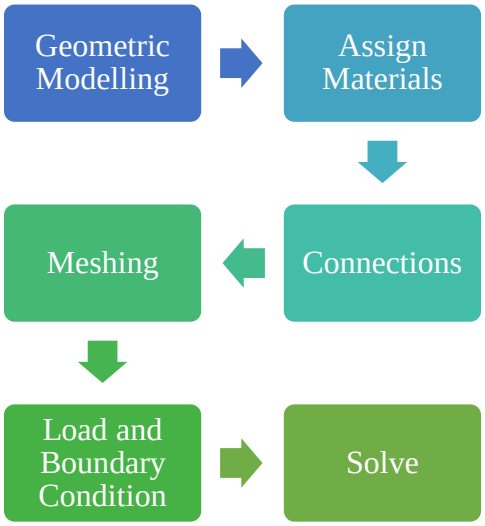

Figure 3 Flow Chart of Modelling

5.1. Geometric Modelling

The wheel and rim were removed from the analysis geometry. The analysis geometry is shown in **Hata! Başvuru kaynağı bulunamadı.**.

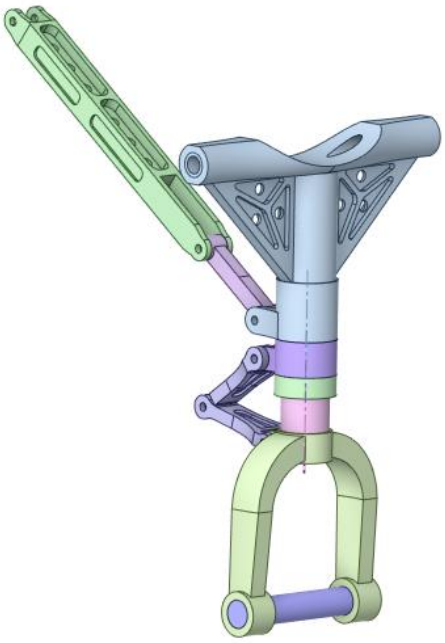

Figure 4 Analysis Geometry

5.2. Assigning Material Properties

Materials were assigned to the components, taking into account the loads on the components and the elasticity and strength of the materials. In some components, different materials were selected and analyzes were made. The information of the materials selected for the components is given in the Table 10.

Table 10. Material Information

Component	Material
Main Strut	AISI 4340
	PH13- 8Mo
	Ti-10V-2Fe-3Al
	Ti-6Al-6V-2Sn
Shock Absorber Cylinder	300M Steel
Fork	AISI 4340
	PH13- 8Mo
	Ti-10V-2Fe-3Al
Torque Links	Al 7075 T6
	Ti 6Al-4V
	AISI 1035
Axle	AISI 4340
Side Stay Arms	Al 7075 T6
	Ti 6Al-4V
	AISI 1035

5.3. Connections

Contact relationships are defined to the connection areas between the components. Pin connections are defined as revolute joints. By determining the bearing areas between the piston and the main strut, the connection is defined as a cylindrical joint. Bolt connections are defined as fixed joints.

5.4. Meshing

Tetrahedral elements are generally used in the three-dimensional model. Hexahedral elements are used in cylindrical structures. Mesh sizes were adjusted by paying attention to the element quality of each component above 0.7. The average element quality of the entire structure is 0.81. The mesh of geometry is shown in the figure.

Figure 5 Mesh of FE Model

5.5. Load and boundary Conditions

In the oleo pneumatic shock absorber, compression in the nitrogen gas was applied as a pressure load. In addition, according to the load calculations, analyzes were made for the three most critical conditions. These forces were applied on the axle as a remote

force from the wheel contact point. The loads for these critical conditions are given in the Table 11.

Table 11. Loads

Case	Condition	Noise Landing Gear Loads (N)		
		Normal Force	Drag Force	Side Force
1	Three point landing with high friction	101085	80868	0
2	Taxing with brake	112310	56155	28077
3	Rolling-back	55225	-38657	0

6. Results

As a result of stress analysis, Von-Mises stresses and deformation results were examined. The stress and deformation results for the three critical conditions of the landing gear system are shared in the figures below. Stress and deformation values caused by material changes on a component basis are shared in the tables.

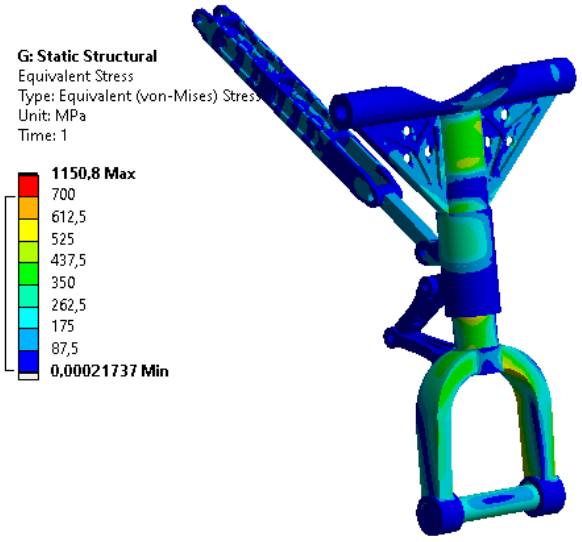

Figure 6 Case 1- Von-Mises Stress

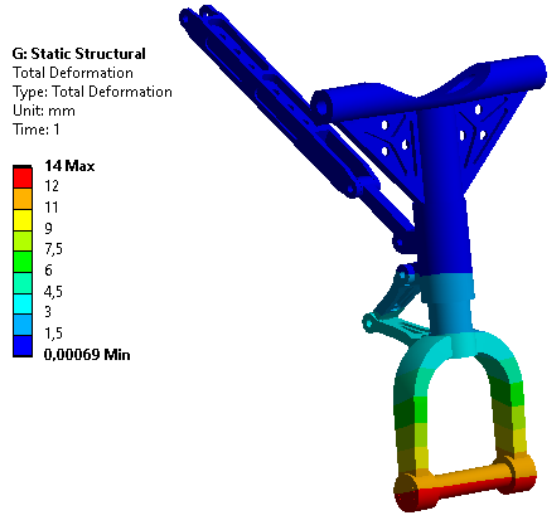

Figure 7 Case 1- Deformation

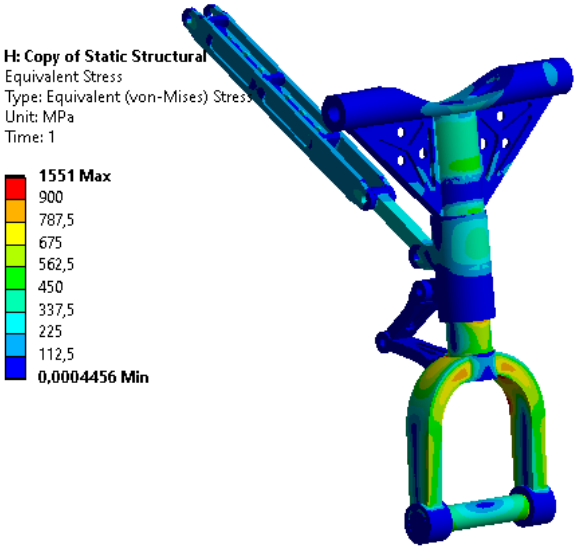

Figure 8 Case 2- Von-Mises Stress

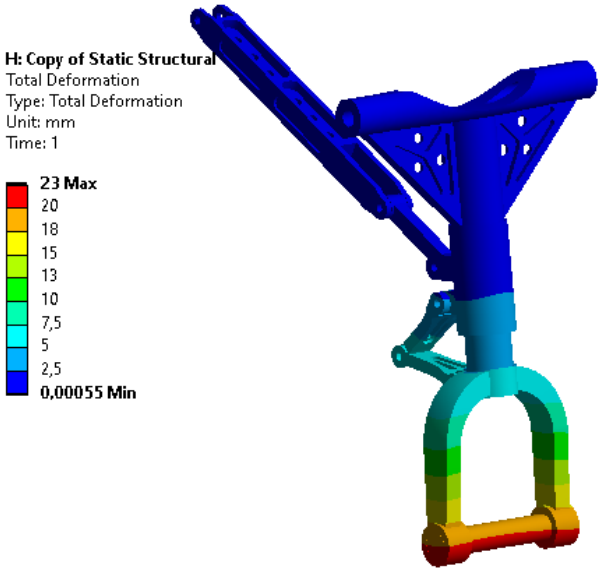

Figure 9 Case 2- Deformation

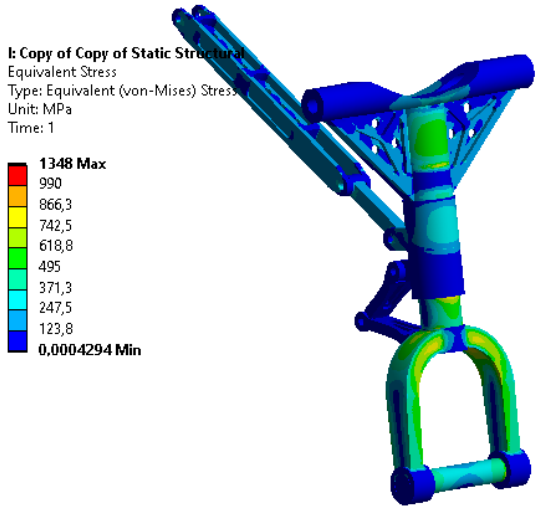

Figure 10 Case 3- Von-Mises Stress

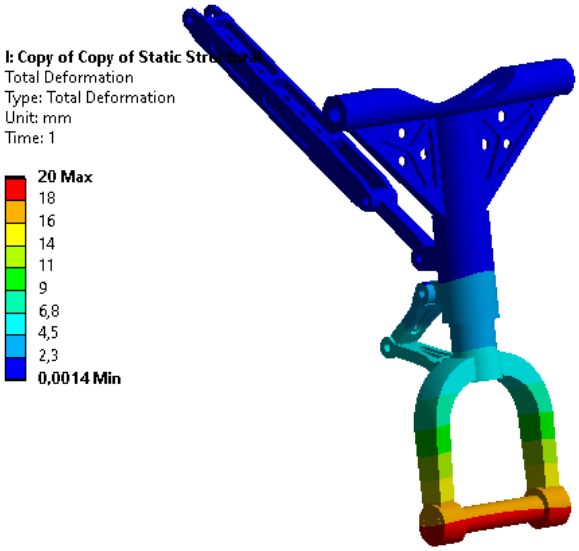

Figure 11 Case 3- Deformation

As a result of the stress analysis, with factor of safety calculations the reliability of the structure is determined. The factor of safety is found by the ratio of the yield stress to the maximum stress. The margin of safety is equal to the factor of safety minus one.

$$\text{Factor of Safety (F.S.)} = \frac{\text{Yield Stress}}{\text{Maximum Stress}}$$

and

$$\text{Margin of Safety (M.S.)} = \frac{\text{Yield Stress}}{\text{Maximum Stress}} - 1$$

6.1. Main Strut

For the main strut, analyzes were made using AISI 4340, PH13-8Mo, Ti-10V-2Fe-3Al, and Ti-6Al-6V-2Sn materials and the results are shared in the Table 12. Since the most critical condition for the main strut is Case 3, the results for Case 3 are compared.

Table 12. Results of Main Strut

Material	Weight (kg)	Max. Stress (MPa)	Deformation (mm)	M.S.
AISI 4340	22.98	798	1.8	0.87
PH13-8Mo	23.28	797	1.7	0.77
Ti-10V-2Fe-3Al	13.88	807	2.4	0.53
Ti-6Al-6V-2Sn	13.55	805	2.4	0.22

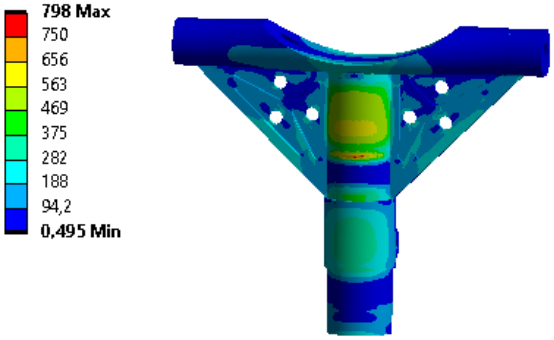

Figure 12 Von-Mises Stress of Main Strut for AISI 4340

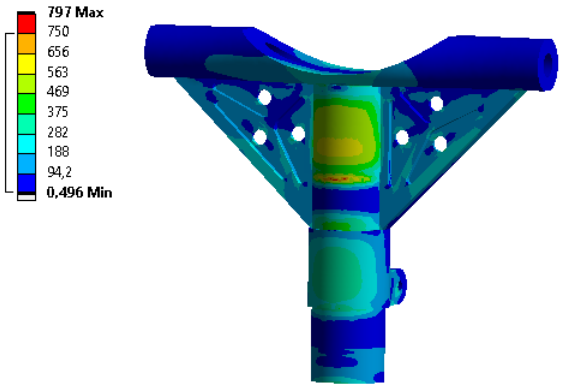

Figure 13 Von- Mises Stress of Main Strut for PH13-8Mo

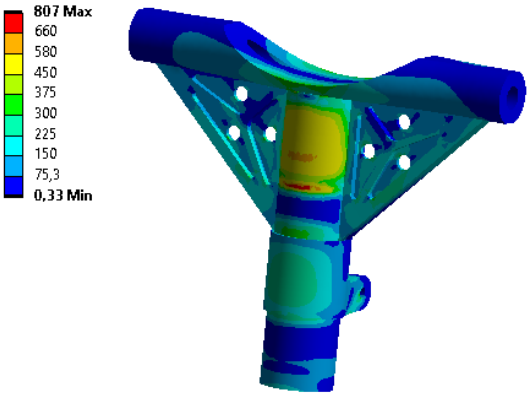

Figure 14 Von- Mises Stress of Main Strut for Ti 10V-2Fe-3Al

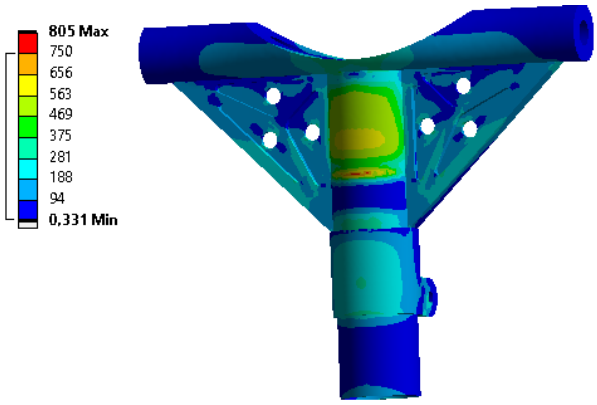

Figure 15 Von- Mises Stress of Main Strut for Ti-6Al-6V-2Sn

6.2. Fork

For the main strut, analyzes were made using AISI 4340, PH13-8Mo and Ti-10V-2Fe-3Al materials and the results are shared in the Table 13. Since the most critical condition for the fork is Case 2, the results for Case 2 are compared.

Table 13. Results of Fork

Material	Weight (kg)	Max. Stress (MPa)	Deformation (mm)	M.S.
AISI 4340	11.93	997	18.3	0.5
PH13-8Mo	12.09	994	17.4	0.42
Ti-10V-2Fe-3Al	7.2	1052	26.12	0.18

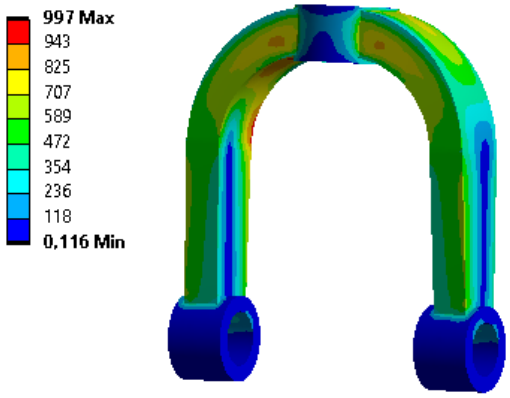

Figure 16 Von-Mises Stress of Fork for AISI 4340

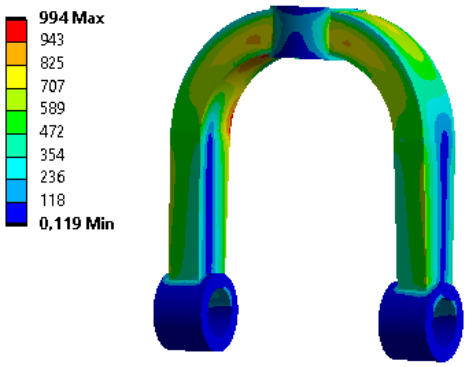

Figure 17 Von-Mises Stress of Fork for PH13-8Mo

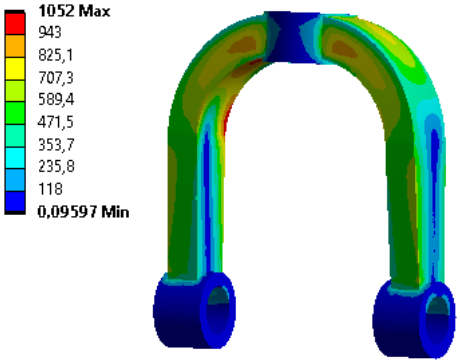

Figure 18 Von-Mises Stress of Fork for Ti-10V-2Fe-3Al

6.3. Torque Links

For the torque links, analyzes were made using Al 7075 T6, Ti 6Al-4V and AISI 1035 materials and the results are shared in the Table 14. Since the most critical condition for the torque links is Case 1, the results for Case 1 are compared.

Table 14. Results of Torque Links

Material	Weight (kg)	Max. Stress (MPa)	Deformation (mm)	M.S.
Al 7075 T6	1.04	47	4	9.7
Ti 6Al-4V	1.64	60	3	13.7
AISI 1035	2.91	86	2.9	5.4

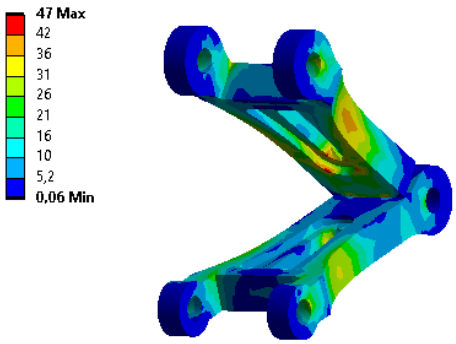

Figure 19 Von-Mises Stress of Torque Links for Al 7075 T6

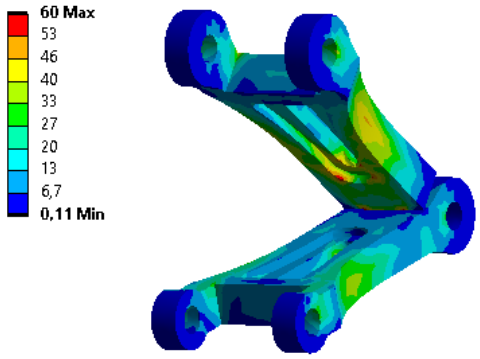

Figure 20 Von-Mises Stress of Torque Links for Al 7075 T6

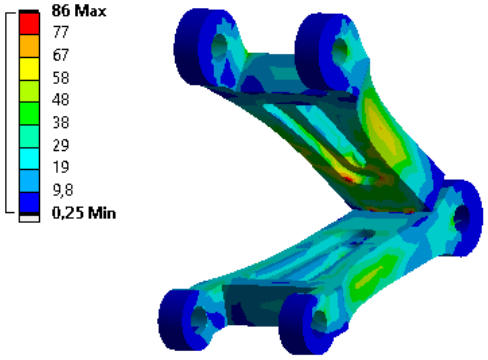

Figure 21 Von-Mises Stress of Torque Links for AISI 1035

6.4. Side Stay Arms

For the side stay arms, analyzes were made using Al 7075 T6, Ti 6Al-4V and AISI 1035 materials and the results are shared in the Table 15. Since the most critical condition for the side stay arms is Case 2, the results for Case 2 are compared.

Table 15. Results of Side Stay Arms

Material	Weight (kg)	Max. Stress (MPa)	Deformation (mm)	M.S.
Al 7075 T6	2.7	429	2.11	0.17
Ti 6Al-4V	4.28	436	1.25	1.02
AISI 1035	7.6	423	0.71	0.3

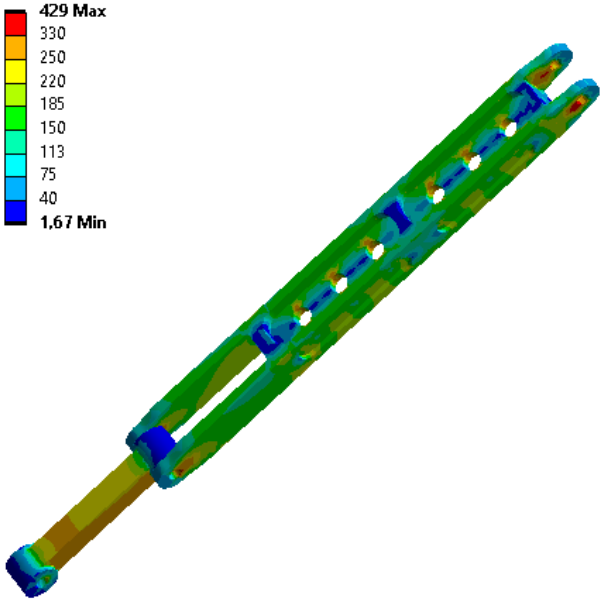

Figure 22 Von-Mises Stress of Side Stay Arms for Al 7075 T6

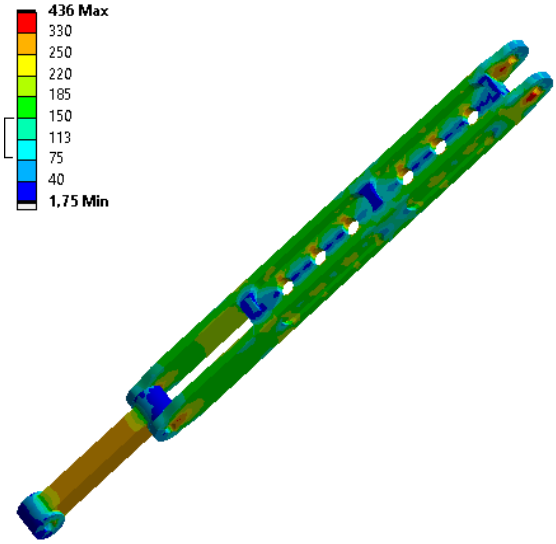

Figure 23 Von-Mises Stress of Side Stay Arms for Ti 6Al-4V

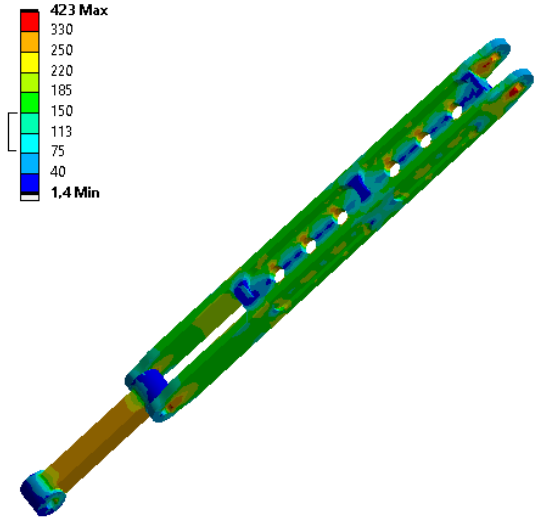

Figure 24 Von-Mises Stress of Side Stay Arms for AISI 1035

6.5. Shock Absorber Cylinder

For the shock absorber cylinder, analyzes were made using 300M Steel the results are shared in the Table 16.

Table 16. Results of Shock Absorber Cylinder

Material	Weight (kg)	Max. Stress (MPa)	Deformation (mm)	M.S.
300M	4	1489	4.8	0.1

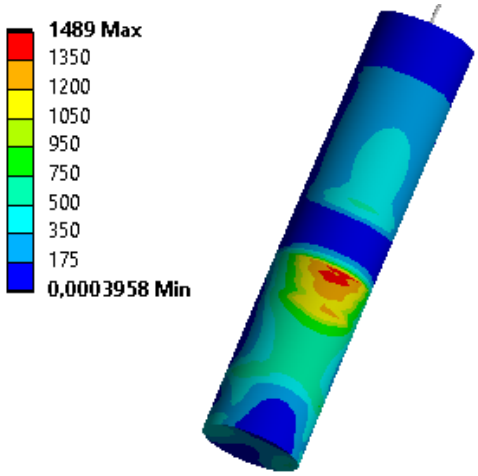

Figure 25 Von-Mises Stress of Shock Absorber Cylinder for 300M

6.5. Axle

For the axle, analyzes were made using AISI 4340 Steel the results are shared in the Table 17.

Table 17. Results of Axle

Material	Weight (kg)	Max. Stress (MPa)	Deformation (mm)	M.S.
AISI 4340	4.1	891	27.1	0.68

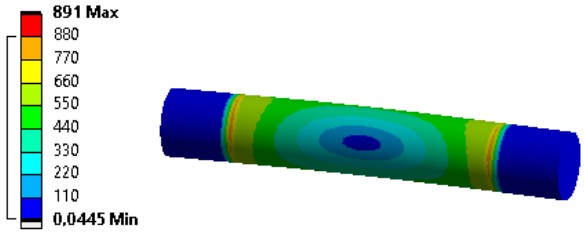

Figure 26 Von-Mises Stress of Axle for AISI 4340

7. Discussion

The accuracy of this study is based on ref. 13 and 14. In both studies, the landing gear was analyzed with the ANSYS program and the structural behavior of titanium alloy 6Al-4V, aluminum alloy 7075 T6 and SAE 1035 steel was investigated. As a result of the studies, it was seen that the lowest deformation was in SAE 1035 steel. Likewise, the same materials were used for the torque links and side stay arms in this study, and the lowest deformation was seen in 1035 steel. Thus, the accuracy of the prepared model is proven. The deformation values and comparison for different materials are shown in

Table 18 and **Hata! Başvuru kaynağı bulunamadı.**.

Table 18 Deformation Comparission

	Deformation (mm)			
Material	**Ref. 13**	**Ref. 14**	**Torque Links**	**Side Stay Arms**
Al 7075 T6	2.82	0.35	4.0	2.11
Ti 6Al-4V	1.77	0.3	3.0	1.01
AISI 1035	1.03	0.25	2.1	0.71

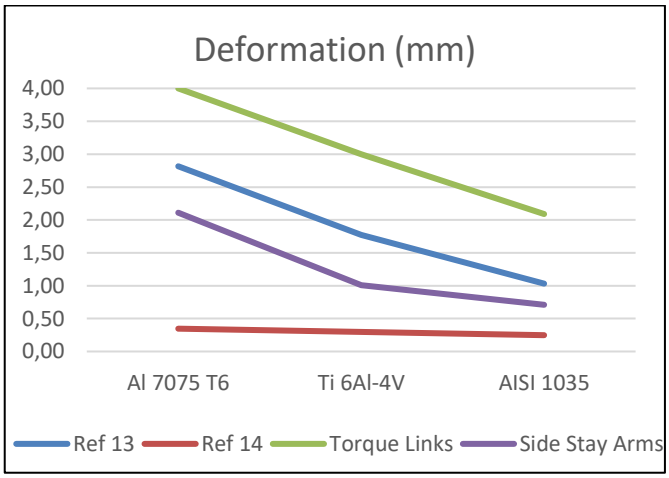

Figure 27 Comparission of Deformation Between Different Materials

4. Conclusions and Recommendations

This study was written with reference to T. D. Nygyen's "Finite Element Analysis of a Nose Gear During Landing" (2010). Structural analysis of the nose landing gear was carried out using the finite element approach. First of all, critical landing conditions were determined and load calculations were made. Then, the contact relationships between the components are defined. Loads were applied as remote force using the method in the reference source. After these processes, the structural analysis of the landing gear system was made for different materials. The results were compared on the basis of parameters such as deformation and stress. Depending on the design requirements, weight, deformation and stress constraints are examined and material changes or design changes can be made in line with the requirements.

References

Arunagiri, P., Vijayakumar, Ayesha Khan, M., & Jani, S.P. (2022). Structural analysis and materials deformations of landing gear. *Materials Today: Proceedings.*

Raymer, D. (2018). Aircraft design: a conceptual approach. American Institute of Aeronautics and Astronautics, Inc.

Basavaraddi, S.R., Manonmani, K.N., & Swami, P. (2015). STRESS AND FATIGUE ANALYSIS OF LANDING GEAR AXLE OF A TRAINER AIRCRAFT. *International Journal of Research in Engineering and Technology, 04, 224-228.*

Conway, H. G. (1958). Landing gear design. Chapman & Hall.

Currey, N. S. (1988). Aircraft landing gear design: principle and practices. AIAA Education Series, Washington, D.C.

Dileep, E., Oblisamy, L., Krithiga, R.S., & Jacob, J. (2016). Structural Analysis of Aircraft Landing Gear During Rough Landing. *International journal of engineering trends and technology, 41, 256-261.*

Jeevanantham, V., Vadivelu, & Manigandan, P. (2017). Material Based Structural Analysis of a Typical Landing Gear.

Gowda, A.C., & Basha, S.N. (2014). Linear Static and Fatigue Analysis of Nose Landing Gear for Trainer Aircraft.

Gudmundsson, S. (2014). General aviation aircraft desing: Applied methods and procedures. ELSEVIER.

Nguyen, T. (2010). FINITE ELEMENT ANALYSIS OF A NOSE GEAR DURING LANDING.

Prasad, V., Reddy, P.K., Rajesh, B., & Sridhar, T. (2020). DESIGN AND STRUCTURAL ANALYSIS OF AIRCRAFT LANDING GEAR USING DIFFERENT ALLOYS. *Internatıonal Journal Of Mechanıcal Engıneerıng And Technology (IJMET).*

Rajesh, A.R., & Bt, A. (2015). Design and Analysis Aircraft Nose and Nose Landing Gear. *Journal of Aeronautics and Aerospace Engineering.*

Raju, M.M., Patan, S. (2017). DESİGN AND STRENGTH ANALYSİS OF NOSE LANDİNG GEAR. *International Journal and Magazine of Engineering, Technology, Management and Research, 04, 71-75.*

Sadraey, M. H. (2013). Aircraft design: A systems engineering approach. John Wiley and Sons.

Schmidt, R. K. (2021). The design of aircraft landing gear R-455. SAE International, 2021.

United States., Battelle Memorial Institute., William J. Hughes Technical Center (U.S.), United States., & United States. (2019). *MMPDS-14: Metallic materials properties development and standardization (MMPDS).*